Organic Frameworks

DOI: 10.1002/ange.201300256

A Squaraine-Linked Mesoporous Covalent Organic Framework**

*Atsushi Nagai, Xiong Chen, Xiao Feng, Xuesong Ding, Zhaoqi Guo, and Donglin Jiang**

Covalent organic frameworks (COFs) are a class of designable crystalline polymers with structural periodicity and inherent porosity.[1–9] COFs have emerged as new porous materials for gas adsorption and storage because of their high porosity, robust thermal stability, and low densities.[1,2,7] In addition, the layered structure of 2D COFs provides periodic arrays of π clouds that can greatly facilitate charge-carrier transport;[1f,3,9] this structural feature is not seen in conventional 1D and 3D polymers. To date, COFs containing boronate ester, boroxine, imine, triazine, and hydrazone linkages have been synthesized.[1–9] The development of new reactions to synthesize such covalent and crystalline frameworks is critical for further progress in this emerging field.

We report herein a new reaction based on squaraine that allows for the synthesis of a new type of 2D COF. Squaraines are interesting dyes with a zwitterionic resonance structure and have broad applications in areas such as imaging, nonlinear optics, photovoltaics, photodynamic therapy, and ion sensing.[10] Squaraines are usually prepared through the condensation of squaric acid (SA) with aromatic, heteroaromatic, or olefinic compounds in a simple one-step reaction.[10] For example, the condensation of SA with *p*-toludine as the donating molecule gives a squaraine (SQ) with a planar yet zigzagged zwitterionic resonance structure (Scheme 1a and b). By using this linkage, we expect to form a conjugated COF with a zigzagged skeleton. We synthesized copper(II) 5,10,15,20-tetrakis(4-aminophenyl)porphyrin (TAP-CuP) as a building block for the SA condensation and constructed a crystalline 2D conjugated COF (CuP-SQ COF; Scheme 1c) with a tetragonal mesoporous skeleton. We demonstrated that the SQ-linked COFs have a zigzagged conformation that protects the layered structure from sideslip, are highly stable in solvents, provide an extended π conjugation over the 2D sheets, and have lower band gap energy and greatly enhanced absorbance capability compared to existing COFs. These features extend the structural and functional scope of COFs.

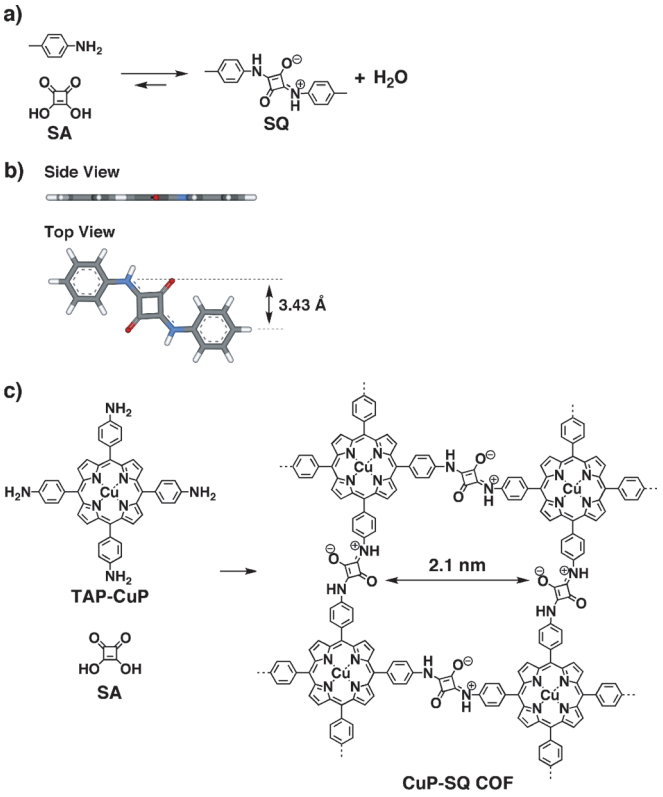

Scheme 1. a) Synthesis of SQ through the condensation of SA with *p*-toludine. b) Side and top view of SQ. C: gray, H: white, N: blue, O: red. c) Synthesis of CuP-SQ COF through the condensation of SA with TAP-CuP.

The CuP-SQ COF was synthesized under solvothermal conditions through the condensation of SA and TAP-CuP in *o*-dichlorobenzene/*n*-butanol (1:1 by vol.) at 85 °C for 7 days. The resulting precipitate was collected by filtration, washed with THF and acetone, and dried at 150 °C under vacuum to provide the CuP-SQ COF as a dark purple powder in 94% yield. When combinations of *n*-butanol with other aromatic solvents, such as mesitylene and 1,3,5-tricholorobenzene, were used, the resulting solid had a lower crystallinity. To investiagte the ratio of *o*-dichlorobenzene to *n*BuOH, ratios of 1:3, 1:2, 1:1, 2:1, and 3:1 were used; the product with the highest crystallinity was obtained when the 1:1 volume ratio was used. The model compound SQ was synthesized under the same reaction conditions in 99% yield (Scheme 1a and the Supporting Information). Thermal gravimetric analysis shows that the CuP-SQ COF is stable up to 300 °C (see the Supporting Information, Figure S1).

The Fourier-transform infrared (FTIR) spectrum of the CuP-SQ COF exhibited a vibration band at 1595 cm^{-1}, characteristic of a C=O bond. This band is blue-shifted relative to SQ (1579 cm^{-1}); this blue shift is most likely due to

[*] Dr. A. Nagai,[+] X. Chen,[+] X. Feng, X. Ding, Dr. Z. Guo, Prof. Dr. D. Jiang
Department of Materials Molecular Science, Institute for Molecular Science, National Institutes of Natural Sciences
5-1 Higashiyama, Myodaiji, Okazaki 444-8787 (Japan)
E-mail: jiang@ims.ac.jp
Prof. Dr. D. Jiang
Precursory Research for Embryonic Science and Technology (PRESTO) (Japan) Science and Technology Agency (JST)
Chiyoda-ku, Tokyo 102-0075 (Japan)
[+] These authors contributed equally to this work.
[**] This work is supported by Precursory Research for Embryonic Science and Technology (PRESTO) (Japan) Science and Technology Agency (JST) (D.J.).
Supporting information for this article is available on the WWW under http://dx.doi.org/10.1002/anie.201300256.

the extended π conjugation of the COF (see the Supporting Information, Figure S2). Elemental analysis of the CuP-SQ COF revealed that the H, C, and N contents were 4.21, 68.22, and 10.77%, respectively, which are close to the calculated values of 3.16, 69.99, and 12.56% expected for an infinite 2D sheet.

Field-emission scanning electron microscopy (FE-SEM) was used to investigate the morphology of the CuP-SQ COF after evaporating a THF suspension on a mica plate. The FE-SEM images indicated the presence of mesoscopic objects (Figure 1a). Dynamic light scattering (DLS) analysis of the COF samples is possible because of their high stability in

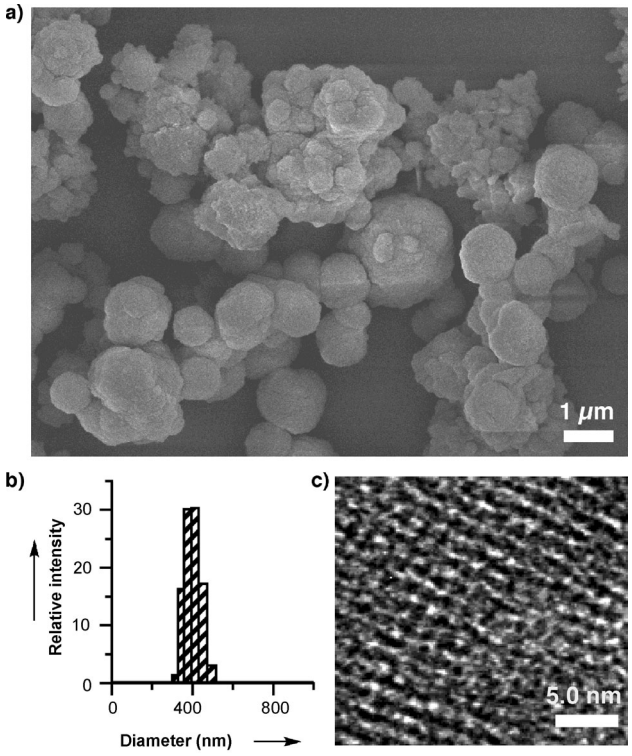

Figure 1. a) FE-SEM image of a typical CuP-SQ COF sample on mica. b) DLS profile of the CuP-SQ COF. c) HR-TEM image of the CuP-SQ COF.

solvents. The size distribution of the COF samples at room temperature in a THF suspension ($c = 0.1\ g\,L^{-1}$) was 371.7 ± 38.4 nm (Figure 1b). High-resolution transmission electron microscopy (HR-TEM) revealed that the CuP-SQ COF has a structure containing regular tetragonal pores (Figure 1c). The tetragonal pores had a width of approximately 2 nm, which is close to the calculated pore size.

CuP-SQ COFs are crystalline materials, as indicated by powder X-ray diffraction (PXRD) measurements. The experimental PXRD pattern displayed a strong peak at 4.16° and relatively weak signals at 8.56 and 21.96°, which were assigned to 100, 200, and 001 facets, respectively (Figure 2a, red curve). The Pawley refined pattern (Figure 2a, blue curve) confirmed the assignment of the observed diffraction peaks (Figure 2a, black curve). The simulation of the PXRD pattern using an AA stacking structure results in a PXRD pattern that

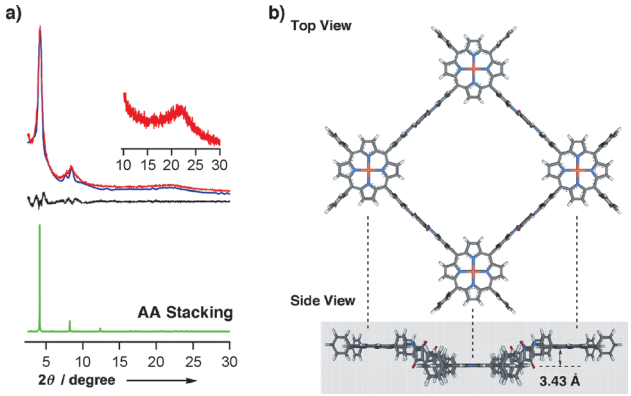

Figure 2. a) PXRD profiles of experimental CuP-SQ COF (red), the Pawley-refined pattern (blue), the difference between these two curves (black), and the simulated pattern for an AA stacking mode (green). b) Top and side views of the tetragonal pore of the CuP-SQ COF.

agreed well with the experimentally observed curve (Figure 2a, green curve). We tried to simulate the PXRD pattern using a staggered stacking mode (AB stacking). However, the AB stacking mode cannot be simulated, because the torsion between the squaraine at the edge and the porphyrin at the nodes of the zigzag-like COF inhibits the staggered stacking of the sheets. These results indicate that the condensation reaction of SA with TAP-CuP forms a 2D CuP-SQ COF that consists of AA-type stacks of the crystalline porphyrin zigzag-like sheets.

SQ is a highly planar molecule without any twists between the phenyl and focal SA units as indicated by the side view of its structure (Scheme 1b). From the top view, it is clear that the two phenyl termini are not located on the longitudinal molecular axis, thus resulting in a zigzagged structure with a 3.43 Å vertical distance between the two phenyl units (Scheme 1b). Consequently, the porphyrin units are also not located on the molecular axis of focal SA units (Figure 2b). This nonlinear alignment gives rise to the 2D zigzag structure. The structural optimization, using Materials Studio, of the elementary tetragonal pore revealed the presence of a higher porphyrin pair and lower porphyrin pair separated vertically by approximately 3.43 Å (Figure 2b). This type of zigzag structure is unprecedented for COFs and, interestingly, helps protect the sheets from sideslip and stabilizes the layered structure.

The porosity of CuP-SQ COF was investigated using its nitrogen sorption isotherm at 77 K. CuP-SQ COFs exhibited a reversible sorption with a typical type IV curve, which indicates a mesoporous character (Figure 3a). The Brunauer–Emmett–Teller (BET) surface area and pore volume were calculated as $539\ m^2\,g^{-1}$ and $0.6410\ cm^3\,g^{-1}$, respectively. The pore-size distribution calculated using the nonlocal density functional theory (NLDFT) was 2.1 nm (Figure 3b), which was identical to the values obatined from the PXRD measurement (2.1 nm) and the theoretical calculations (2.1 nm). These results indicate that the condensation reaction forms a SQ-linked COF with porphyrin nodes and SQ bridges in a mesoporous tetragonal 2D framework. The theoretical simulation of the BET surface area gives a value of

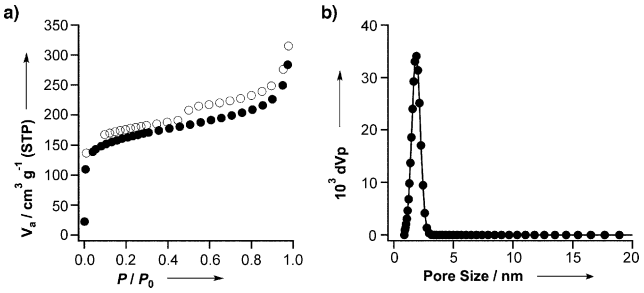

Figure 3. a) Nitrogen sorption isotherm curves measured at 77 K, black circles: desorption, white circles: adsorption. b) Pore-size distribution profile.

2289 $m^2 g^{-1}$ with a pore size of 2.1 nm. The surface area of CuP-SQ COF is related to the size of its microcrystals, a trend that is also observed for boronate-linked and other COFs.[3d,i]

From a structural perspective, this CuP-SQ COF is unique because of the multiplicity in the porous skeleton. First, the CuP-SQ COF has a zwitterionic structure that allows resonance conjugation between the porphyrin and SQ units. Second, the CuP-SQ COF has an unconventional zigzag structure and a flat and twisted 2D layer structure. Third, the walls of a single layer of the CuP-SQ COF are not on the same plane because of the zigzag structure, thus producing bowl-shaped pores. Finally, electrochemical studies show that the CuP-SQ COF has an electron-deficient skeleton, which may allow two-directional electron flow through the stacked column and over the 2D plane.[3f,h]

UV–Vis absorption spectroscopy was used to evaluate the electronic properties of the CuP-SQ COF relative to TAP-CuP and SQ. The CuP-SQ COF exhibited a Soret band at 467 nm (Figure 4, red curve), which was red-shifted by over 28 nm relative to that of TAP-CuP (black curve) and at least 100 nm from the band exhibited by SQ (dotted curve). The extremely broadened Soret band of CuP-SQ COF suggests a delocalization of the π electrons in the COF. The order of the band gaps as estimated from the onset wavelength in the UV–Vis absorption spectra was as follows: SQ (2.6 eV) > TAP-CuP (1.9 eV) > CuP-SQ COF (1.7 eV). This significant bathochromic shift and narrow band gap indicate an extended π conjugation over the 2D skeletons of the COF.

In addition, the Q bands of CuP-SQ COF were observed at 560 and 605 nm with a significant extension to 750 nm. Interestingly, the CuP-SQ COF possessed drastically

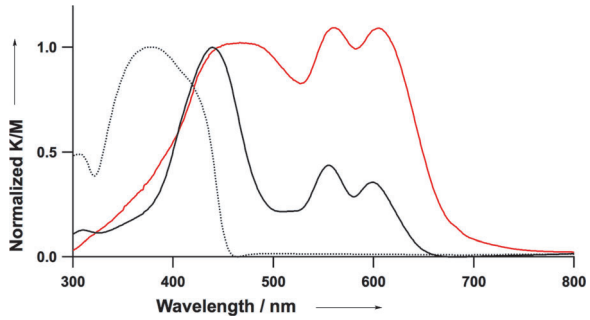

Figure 4. Absorption spectra of the CuP-SQ COF (red curve), TAP-CuP (black curve), and SQ (dotted curve).

enhanced absorption for both deep-red visible and near-infrared photons. The CuP-SQ COF exhibited relative intensity ratios for the Q band versus the Soret band (I_{605nm}/I_{Soret}) as high as 1.1. In sharp contrast, TAP-CuP has an I_{605nm}/I_{Soret} value of only 0.38. Such an enhancement in the Q-band absorption has been observed for metallophthalocyanine COFs.[3c] These results indicate that the stacked porphyrin structure of the 2D COF enhances its absorption capability in the long-wavelength visible and near-infrared regions. Usually, porphyrin chromophores exhibit strong absorption bands only in a narrow visible zone around 420 nm. In contrast, the CuP-SQ COFs can harvest a wide range of photons from the visible to deep-red regions. The broadened and red-shifted Soret band together with the enhanced Q band almost doubles the light-absorbing capability of the CuP-SQ COF relative to the monomeric CuP. These outstanding π-electronic properties originate from the intersheet π conjugation and well-defined intrasheet stacking structure in the CuP-SQ COF.

The electrochemical behavior of both the CuP-SQ COF and TAP-CuP was studied by the cyclic voltammetry (CV) of a DMF suspension ($c = 1.0\ g\,L^{-1}$; see the Supporting Information, Figure S3). The CV curves were recorded using an Ag/Ag^+ (0.01 mol L^{-1} BuN_4F_6P in DMF) electrode calibrated using the Fc/Fc^+ redox coupling (4.4 eV below the vacuum level). Both the CuP-SQ COF and TAP-CuP exhibited three reduction peaks; however, no clear oxidation peaks were observed. The lowest unoccupied molecular orbital (LUMO) of the CuP-SQ COF was estimated from the onset of reduction potential as −4.0 eV (see the Supporting Information, Figure S4), which is close to that of TAP-CuP (−4.1 eV). However, the CuP-SQ COF had a highest occupied molecular orbital (HOMO) of −5.7 eV, which is higher than that of TAP-CuP (−6.0 eV) estimated using the LUMO level and the band gap. The higher HOMO energy level of the CuP-SQ COF means that the π electrons are more delocalized in the 2D COF skeleton than in the large π macrocycle TPA-CuP, that is, the π conjugation was extended over the 2D COF skeletons.

Stability is an important parameter for the crystalline COFs. We tested the stability of the CuP-SQ COF by dispersing the sample in different solvents for 24 h and measuring their PXRD patterns after vacuum drying. As shown in Figure S5 (see the Supporting Information), the COF samples are stable; there is no change in their PXRD patterns and they retain their crystallinity in common organic solvents, such as methanol, benzene, and hexane, irrespective of their polarity, and even in water and aqueous HCl solution (1M). In contrast, the boronate- and boroxine-linked COFs, which do not have a π conjugated skeleton, do not keep the crystalline structure upon exposure to water, alcohol, and acid.

Based on these findings, we explored the possibility of using the CuP-SQ COF as a heterogeneous catalyst. By virtue of its conjugated structure, the CuP-SQ COF can harvest visible photons for photocatalytic reactions. Indeed, the CuP-SQ COF is an excellent photocatalyst for the activation of molecular oxygen (see the Supporting Information). The generation of singlet oxygen was investigated using the well-

established 1,3-diphenylisobenzofuran (DPBF) as a label and was monitored by time-dependent electronic absorption spectroscopy.[11] As shown in Figure 5a, the visible light irradiation of an oxygen-saturated DMF solution (2.3 mL) of DPBF (50 μM) in the presence of CuP-SQ COF (0.1 mg) caused a steady conversion of molecular oxygen into singlet oxygen, as evident by the spectral change with clear isosbestic

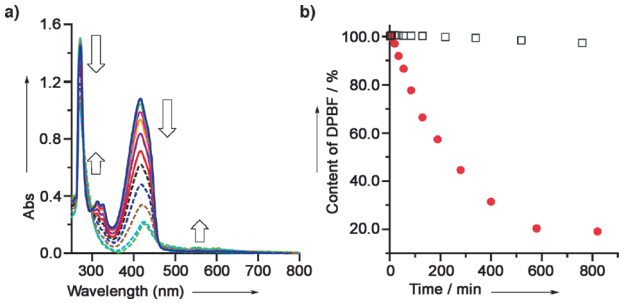

Figure 5. a) Absorption spectra of DPBF in the presence of CuP-SQ COF in DMF on irradiation at 500 nm. Arrows indicate the change of absorbance from 0 to 819 min upon irradiation with light. b) Plot of the DPBF content in the systems (black: CuP; red: CuP-SQ COF) versus the irradiation time.

points. In sharp contrast, the monomeric CuP showed low catalytic activity for the same reaction, thus giving rise to only very small spectral change (see the Supporting Information, Figure S6). The plot of time against the content of DPBF showed that in the presence of the CuP-SQ COF the amount of DPBF decreased rapidly, whereas for the system containing monomeric CuP the reaction was very sluggish (Figure 5b). Generation of singlet oxygen requires the triplet state of a photosensitizer. Therefore, we can conclude that the CuP-SQ COF, upon the absorption of visible photons, can efficiently generate the triplet excited state that triggers the activation of molecular oxygen. The significant difference in the catalytic abilities of monomeric CuP and CuP-SQ COF also indicates that owing to the well-defined ordered structure the COF architecture is useful for controlling the photogenerated excited states. Metalloporphyrins containing nobel metals such as palladium and platinum, have been extensively studied for the activation of molecular oxygen because of their high efficiency in generating the triplet state. CuP-SQ COF, which contains no nobel metals, opens a new avenue for this fundamental yet still challenging photocatalytic reaction.

In summary, we have developed a new reaction for COF synthesis based on squaraine chemistry. A high-throughput protocol was established for the condensation reaction of SA with porphyrin. The SQ-linked COF features high crystallinity, inherent porosity, and robust solvent stability. The SQ linkage is unique because it extends the π conjugation over the 2D skeleton and provides a new molecular motif for charge-carrier transfer. Their improved light-harvesting capacity, lowered band gap, layered π-stacking porphyrin arrays, and open mesopores are useful features for the development of functional molecular systems, for example, photocatalytic systems. This research expands the scope of COFs and constitutes an important step toward porous crystalline organic architecture with designed π conjugation and functions.

Received: January 11, 2013
Published online: February 21, 2013

Keywords: conjugation · covalent organic frameworks · photocatalyst · porphyrinoids · synthetic methods

[1] a) A. P. Cote, A. I. Benin, N. W. Ockwig, M. O'Keeffe, A. J. Matzger, O. M. Yaghi, *Science* **2005**, *310*, 1166–1170; b) H. M. El-Kaderi, J. R. Hunt, J. L. Mendoza-Cortés, A. P. Côté, R. E. Taylor, M. O'Keeffe, O. M. Yaghi, *Science* **2007**, *316*, 268–272; c) A. P. Côté, H. M. El-Kaderi, H. Furukawa, J. R. Hunt, O. M. Yaghi, *J. Am. Chem. Soc.* **2007**, *129*, 12914–12915; d) J. R. Hunt, C. J. Doonan, J. D. LeVangie, A. P. Côté, O. M. Yaghi, *J. Am. Chem. Soc.* **2008**, *130*, 11872–11873; e) C. J. Doonan, D. J. Tranchemontagne, T. G. Glover, J. R. Hunt, O. M. Yaghi, *Nat. Chem.* **2010**, *2*, 235–238; f) S. Wan, F. Gndara, A. Asano, H. Furukawa, A. Saeki, S. K. Dey, L. Liao, M. W. Ambrogio, Y. Y. Botros, X. Duan, S. Seki, J. F. Stoddart, O. M. Yaghi, *Chem. Mater.* **2011**, *23*, 4094–4097; g) F. J. Uribe-Romo, C. J. Doonan, H. Furukawa, K. Oisaki, O. M. Yaghi, *J. Am. Chem. Soc.* **2011**, *133*, 11478–11481.

[2] a) R. W. Tilford, W. R. Gemmill, H. C. zur Loye, J. J. Lavigne, *Chem. Mater.* **2006**, *18*, 5296–5301; b) R. W. Tilford, S. J. Mugavero, P. J. Pellechia, J. J. Lavigne, *Adv. Mater.* **2008**, *20*, 2741–2746; c) L. M. Lanni, R. W. Tilford, M. Bharathy, J. J. Lavigne, *J. Am. Chem. Soc.* **2011**, *133*, 13975–13983.

[3] a) X. Feng, X. Ding, D. Jiang, *Chem. Soc. Rev.* **2012**, *41*, 6010–6022; b) A. Nagai, Z. Guo, X. Feng, S. Jin, X. Chen, X. Ding, D. Jiang, *Nat. Commun.* **2011**, *2*, 536; c) S. Wan, J. Guo, J. Kim, H. Ihee, D. Jiang, *Angew. Chem.* **2008**, *120*, 8958–8962; *Angew. Chem. Int. Ed.* **2008**, *47*, 8826–8830; d) S. Wan, J. Guo, J. Kim, H. Ihee, D. Jiang, *Angew. Chem.* **2009**, *121*, 5547–5550; *Angew. Chem. Int. Ed.* **2009**, *48*, 5439–5442; e) X. Ding, J. Guo, X. Feng, Y. Honsho, J. D. Guo, S. Seki, P. Maitarad, A. Saeki, S. Nagase, D. Jiang, *Angew. Chem.* **2011**, *123*, 1325–1329; *Angew. Chem. Int. Ed.* **2011**, *50*, 1289–1293; f) X. Ding, L. Chen, Y. Honso, X. Feng, O. Saengsawang, J. D. Guo, A. Saeki, S. Seki, S. Irle, S. Nagase, V. Parasuk, D. Jiang, *J. Am. Chem. Soc.* **2011**, *133*, 14510–14513; g) X. Feng, L. Chen, Y. P. Dong, D. Jiang, *Chem. Commun.* **2011**, *47*, 1979–1981; h) X. Feng, L. Liu, Y. Honsho, A. Saeki, S. Seki, S. Irle, Y. P. Dong, A. Nagai, D. Jiang, *Angew. Chem.* **2012**, *124*, 2672–2676; *Angew. Chem. Int. Ed.* **2012**, *51*, 2618–2622; i) X. Feng, L. Chen, Y. Honsho, O. Saengsawang, L. Liu, L. Wang, A. Saeki, S. Irle, S. Seki, Y. P. Dong, D. Jiang, *Adv. Mater.* **2012**, *24*, 3026–3031; j) X. Ding, X. Feng, A. Saeki, S. Seki, A. Nagai, D. Jiang, *Chem. Commun.* **2012**, *48*, 8952–8954; k) X. Feng, Y. P. Dong, D. Jiang, *CrystEngComm* **2013**, *15*, 1508–1511; l) X. Chen, M. Addicoat, S. Irle, A. Nagai, D. Jiang, *J. Am. Chem. Soc.* **2013**, *135*, 546–549; m) S. Jin, X. Ding, X. Feng, M. Supur, K. Furukawa, S. Takahashi, M. Addicoat, M. E. El-Khouly, T. Nakamura, S. Irle, S. Fukuzumi, A. Nagai, D. Jiang, *Angew. Chem.* **2013**, *125*, 2071–2075; *Angew. Chem. Int. Ed.* **2013**, *52*, 2017–2021.

[4] a) P. Kuhn, M. Antonietti, A. Thomas, *Angew. Chem.* **2008**, *120*, 3499–3502; *Angew. Chem. Int. Ed.* **2008**, *47*, 3450–3453; b) M. J. Bojdys, J. Jeromenok, A. Thomas, M. Antonietti, *Adv. Mater.* **2010**, *22*, 2202–2205.

[5] N. L. Campbell, R. Clowes, L. K. Ritchie, A. I. Cooper, *Chem. Mater.* **2009**, *21*, 204–206.

[6] a) E. L. Spitler, W. R. Dichtel, *Nat. Chem.* **2010**, *2*, 672–677; b) J. W. Colson, A. R. Woll, A. Mukherjee, M. P. Levendorf, E. L. Spitler, V. B. Shields, M. G. Spencer, J. Park, W. R. Dichtel,

Science **2011**, *332*, 228 – 231; c) E. L. Spitler, B. T. Koo, J. L. Novotney, J. W. Colson, F. J. Uribe-Romo, G. D. Gutierrez, P. Clancy, W. R. Dichtel, *J. Am. Chem. Soc.* **2011**, *133*, 19416 – 19421; d) E. L. Spitler, J. W. Colson, F. J. Uribe-Romo, A. R. Woll, M. R. Giovino, A. Saldivar, W. R. Dichtel, *Angew. Chem.* **2012**, *124*, 2677 – 2681; *Angew. Chem. Int. Ed.* **2012**, *51*, 2623 – 2627; e) D. N. Bunck, W. R. Dichtel, *Angew. Chem.* **2012**, *124*, 1921 – 1925; *Angew. Chem. Int. Ed.* **2012**, *51*, 1885 – 1889; f) B. T. Koo, W. R. Dichtel, P. Clancy, *J. Mater. Chem.* **2012**, *22*, 17460 – 17469.

[7] M. Dogru, A. Sonnauer, A. Gavryushin, P. Knochel, T. Bein, *Chem. Commun.* **2011**, *47*, 1707 – 1709.

[8] S. Y. Ding, J. Gao, Q. Wang, Y. Zhang, W. G. Song, C. Y. Su, W. Wang, *J. Am. Chem. Soc.* **2011**, *133*, 19816 – 19822.

[9] S. Patwardhan, A. A. Kocherzhenko, F. C. Grozema, L. D. A. Siebbeles, *J. Phys. Chem. C* **2011**, *115*, 11768 – 11772.

[10] W. Ziegenbein, H. E. Sprenger, *Angew. Chem.* **1966**, *78*, 937 – 937; *Angew. Chem. Int. Ed.* **1966**, *5*, 893 – 894.

[11] S. Wolfgang, K. Holger, W. Dieter, H. Steffen, R. Beate, S. Gunter, *J. Porphyrins Phthalocyanines* **1998**, *2*, 145 – 158.